

# Effects of targeting pod modification on F/A-18C Hornet weapons release

**C. W. O'Brien and M. R. Snyder**

Department of Mechanical Engineering,  
United States Naval Academy (USNA)  
Annapolis, USA

**E. N. Hallberg**

Department of Aerospace Engineering, USNA  
Annapolis, USA

**A. Cenko**

Store Separation Consultant, Dunkirk  
Maryland, USA

## ABSTRACT

This paper describes a study that investigated the efficacy of modifications to the trailing end of the externally mounted advanced targeting forward looking infrared pod (ATFLIR) on the store separation characteristics of the F/A-18C aircraft. Prior work by Godiksen suggests that the trailing end of the geometrically similar targeting forward looking infrared pod (TFLIR) is the likely source of shock waves that can adversely impact the trajectory of a recently released store. In our study five different modifications to the aft end of the ATFLIR were analysed using computational fluid dynamics (CFD). The two most promising designs, an ogive shape such as that used in artillery shells and rockets, and a simpler extended but truncated cone shape were then further investigated. The moments that these trailing shapes produced on an adjacent released store were compared. CFD analysis revealed that the simpler cone shape resulted in weaker shocks from the aft end of the pod with a resultant smaller adverse moment on the store. While there is an extensive history of using CFD to predict store separation behavior, results from our study should be compared with wind tunnel data in order to validate the CFD simulations.

## NOMENCLATURE

6-DOF	six-degree of freedom
AOA	angle-of-attack
ATFLIR	advanced targeting forward looking infrared pod
$C_d$	drag coefficient
CFD	computational fluid dynamics

$Cm_x$	$x$ direction moment coefficient
$Cm_y$	$y$ direction moment coefficient
$Cm_z$	$z$ direction moment coefficient
F/A-18C	US Navy and Allied fighter attack aircraft
GBU	glide bomb unit
IFM	influence function method
JDAM	joint direct attack munition
Mk-82	500lb gravity bomb
Mk-83	1,000lb gravity bomb
Mk-84	2,000lb gravity bomb
PSP	pressure sensitive paint
S-3B	USN carrier based high wing multi-purpose aircraft
SLAM-ER	Standoff land attack missile – expanded response
TFLIR	targeting forward looking infrared pod
TTCP	The Technical Cooperative Program
USNA	United States Naval Academy

## 1.0 INTRODUCTION

In order to establish safe flight conditions for the release of bombs or other stores from attack aircraft, the US Navy conducts flight tests at various aircraft attitudes, Mach numbers and store configurations and determines the initial path taken by the falling store. This determination of path is generally made using a series of high speed photographs, known as photogrammetrics, or the analysis of data taken from an accelerometer located on the store itself, known as telemetry. Though very accurate, many such flight tests are necessary in order to approve a range of acceptable flight conditions, and these are costly in both time and money. In the absence of pre-flight analysis, the most benign flight condition is chosen as the starting point of the flight test, typically fully subsonic. The release envelope is gradually expanded through subsequent releases by increasing the Mach and altitude. Many such flights are required to reach the boundary of the aircraft flight envelope.

The number and duration of flights required can be significantly reduced by predicting trajectories before flights are begun. This pre-flight flow analysis is accomplished in both the wind tunnel and through computational fluid dynamics (CFD). Prior to any flight testing, predicted trajectories are obtained using one or both of these methods, and these results are used to determine which configurations require flight tests and to what extent. For instance, a clearance to Mach 0.95 may require a build-up approach beginning at a benign flight condition such as Mach 0.80 and progressing up to Mach 0.95 at incremental steps of Mach 0.05. Extensive wind tunnel and CFD analysis could permit fewer steps in the build-up to the endpoint if CFD and wind tunnel analysis shows the endpoint to be safe, and interim flight test steps match predictions.

## 2.0 BACKGROUND

The basis for this research began with routine bombing practice conducted in Fallon, Nevada in December 1998. The pilot was flying an F/A-18C aircraft with a targeting forward looking infrared pod (TFLIR) mounted on the side of the plane's fuselage and a Mk-82 500lb bomb hanging from the inboard wing pylon adjacent to the targeting pod. Figure 1 shows an F/A-18C aircraft with a TFLIR attached to the fuselage and a fuel tank attached to the inboard pylon.

When the pilot released the Mk-82 from his aircraft, the nose of the bomb yawed away from the fuselage which caused the bomb's tail fins to impact the TFLIR. This result was unexpected as this flight condition had been cleared for safe release in the aircraft's tactical manual. An investigation soon revealed that the TFLIR had been considered a part of the aircraft and that its effect on store separation had been assumed to be negligible. As a result, neither wind tunnel nor flight testing had been done to determine what affect the TFLIR might have on store release. After this incident, the U.S. Navy began a flight test program in order to establish safe release parameters. As will be discussed in a following section, analysis by Godiksen<sup>60</sup> showed that CFD could be useful in predicting stores release behaviour on the F/A-18C equipped with the TFLIR pod.

At this same time the Navy introduced the advanced targeting forward looking infrared pod (ATFLIR), which is geometrically similar to the TFLIR but significantly more capable. Figure 2 shows an ATFLIR mounted on an F/A-18C. The main difference in shape between these two pods is the fairing on the leading end of the ATFLIR, which is not present on the TFLIR. In most other aspects, these pods look essentially identical. There are subtle differences in the geometry of the trailing end of the pods which were initially thought to be insignificant compared to the larger differences in their front-end geometries. This assumption was later shown to be incorrect.

This pod was examined in the flight test program in the same manner as the TFLIR. It was expected that the ATFLIR would have nearly the same effect on the aircraft's flow field as the TFLIR due to their geometric similarity. However, flight test results soon proved otherwise. At speeds just under the speed of sound, between Mach 0.90 and 0.95, the flight test results showed significant differences in the trajectories of bombs dropped next to the TFLIR versus those beside the ATFLIR. Although the cause of this variance was not understood, time and schedule constraints precluded further research. The flight test program concluded by restricting the release of certain stores in proximity to either targeting pod to a subset of the full combat aircraft flight envelope.

While these test flights were successful in establishing safe store release conditions for these pods, they did not produce a full understanding of the effect of the (A)TFLIR pod on the F/A-18C flow field. Furthermore, the full operating envelope of the combat aircraft was restricted. Analysis of this release condition is challenging. The geometric differences between the two pods are subtle and the flow field at the Mach of interest is fully transonic with a number of shocks forming and moving as the store is released. CFD may allow for a detailed investigation of the affect of different ATFLIR aft section geometries on store separation.

### 3.0 LITERATURE REVIEW

Attempts to determine aircraft store separation characteristics using numerical methods date from the late 1970s and early 1980s, where simple codes (e.g. 1,000 panels) were used to provide a solution for an external store on an aircraft<sup>24</sup>. These codes were very limited and were not accepted by wind tunnel and flight test engineers as validated tools to determine store separation characteristics<sup>69</sup>.

During the 1980s, as computational capabilities improved significantly, more advanced CFD simulations, such as the influence function method (IFM)<sup>67</sup>, were developed to help determine loads and moments for external stores. The IFM method used CFD to determine the aircraft flow field which was used to quantify the impact of the flow field on stores, with resultant store aerodynamic coefficients applied to determine store trajectories with a six-degree-of-freedom (6-DOF) programme. This was a one-way coupling method where store modification of the aircraft flow field was not evaluated.

During the 1990s extensive efforts were made to validate and accelerate the use of CFD in the store certification process. Four major international conferences were completed that attempted



Figure 1. TFLIR (left) on F/A-18C.



Figure 2. ATFLIR on F/A-18C.

to validate the use of CFD in the store separation and certification process<sup>6</sup>. During the Applied CFD Challenge II<sup>6</sup>, comparison of eight different CFD simulations with both wind tunnel and flight test data were made for an F/A-18C equipped with a joint direct attack munition (JDAM) Mk-84 2,000lb gravity bomb in a 45° dive at Mach = 0.962 and 1.05. Excellent correlation was shown by the different CFD simulations with both wind tunnel and flight test data,<sup>6</sup> though there were questions about the simulations using JDAM canards, with unexpectedly similar results obtained for simulations with and without the canards<sup>6</sup>.

Another significant study, under the auspices of The Technical Cooperative Program (TTCP – co-operative research program involving the governments of the United States, United Kingdom, Canada, Australia and New Zealand ), was of an F/A-18C releasing a Mk-83 1,000lb gravity bomb. In this study comparison was made between wind tunnel pressure sensitive paint (PSP) data as well as flight test store trajectories<sup>6,10</sup>. CFD simulations were performed using the NASA USM3d flow solver, which is part of the Tetrahedral Unstructured Software System (TetrUSS)<sup>12,15</sup> and with SPLITFLOW, a Lockheed Martin Aeronautics Company propriety code<sup>16,17</sup>. Both codes exhibited excellent comparison with observed wind tunnel PSP pressure distributions and moments, and in predicted versus observed flight test trajectories.

During the 2000s, the use of CFD for predicting external store separation behaviour has reached a comparatively mature phase, with advanced CFD codes being used to improve the design process on new aircraft such as the Joint Strike Fighter and Boeing PA-8<sup>8</sup>. CFD was used successfully to obtain flight clearance for a F/A-18C with a GBU-12 (Mk-82 500lb gravity bomb with added glide bomb unit consisting of nose-mounted laser or GPS seeker plus tail fins for guidance) attached to an under wing canted vertical ejector rack outboard of a 330USG external fuel tank<sup>9</sup>. Additionally, excellent correlation was obtained between CFD predictions and flight tests for the GBU-31, GBU-32 and GBU-38 (GPS guided Mk-84, Mk-83 and Mk-82 gravity bombs)<sup>18</sup>. CFD was also used to determine safe separation flight envelopes for the release of the standoff land attack missile – expanded response (SLAM-ER) from a S-3B carrier-based high-wing multi-purpose aircraft<sup>19</sup>.

This analysis combined CFD solutions for aircraft and stores interference flow fields with 6-DOF trajectory simulation software to predict released store trajectories. The CFD code employed was OVERFLOW<sup>20</sup>, an overset grid code, which uses the Spalart-Allmaras single equation turbulence model<sup>21</sup>. Because of good correlation between CFD/6-DOF and flight test results, two of five planned flight test points for store certification were eliminated. However, the S-3B SLAM-ER simulations and the flight testing performed were both limited to subsonic (Mach < 0.8) conditions, which do not exhibit problematic transonic shock waves. However, in subsequent

work by Godiksen<sup>10</sup>, simulations using USM3d of transonic shock waves at Mach = 0.8 and 0.95 interacting with released stores approximately matched flight test results.

Most examples, including those previously discussed, of the successful application of CFD to stores separation analysis have been limited to aircraft modifications involving placement of stores in a different location from what was previously cleared through extensive flight test and wind tunnel testing. There is little published evidence, however, concerning the validation of CFD analyses of new store designs on existing aircraft, existing store designs on new aircraft, new store designs on new aircraft, or the behaviour of stores released from an internal cavity<sup>6,22</sup>.

It is important to note that wind tunnel testing can have separate errors that can cause disparities between wind tunnel data and CFD simulations. Wind tunnel testing of stores involves the use of stings which are assumed to not produce moments on the store, though there is some data that suggest this is not always the case<sup>23,24</sup>. Wind tunnels also exhibit blockage effects, which are not present in flight test nor usually modeled by CFD.

## 4.0 USE OF NASA USM3D IN STORE SEPARATION ANALYSIS

USM3d is one of several advanced CFD codes that have been used in store separation analysis. As mentioned previously, it was used successfully in the Applied CFD Challenge II<sup>10</sup> and in the TTCP F/A-18C/Mk-83 study<sup>10,11</sup>. This section will discuss other more recent applications of USM3d in store separation analysis.

Godiksen<sup>25</sup> used USM3d to complete a detailed study of the effects of different external targeting pods, specifically the TFLIR, ATFLIR and Litening, on the store separation characteristics of the F/A-18C. In this study Godiksen shows good comparison between CFD simulations and wind tunnel testing for an F/A-18C in a clean configuration (no pods or stores) for flow up wash and side wash angles at various points in the flow for both Mach 0.8 and 0.95. Godiksen completed separate CFD simulations of a GBU-31 at Mach 0.95 and compared resultant forces and moments with wind tunnel data for angle-of-attacks (AOA) between  $-20^\circ$  and  $30^\circ$ . Comparisons were very close except for some variation around  $15^\circ$  AOA. Godiksen speculated that the difference there may have arisen from the CFD failing to capture the effect of vortices generated by body strakes impacting tail fins, or by interference effects of the test apparatus in the wind tunnel. Simulations of the impact of the clean and ATFLIR equipped F/A-18C on the released GBU-31 were completed using USM3d and then compared with available flight test data. Comparison of horizontal and vertical position data showed good correlation for the first 0.2 seconds after release. Predicted horizontal displacement diverged after 0.2 seconds, though vertical displacement tracked well for the 0.4 second after release period evaluated. CFD and flight test data for yaw and pitch angle track closely for the first 0.3 seconds after release, and then increasingly diverged. Godiksen noted, however, that the flight test data was taken using cameras on an aircraft flying abeam of the aircraft releasing the store, with resultant less accurate readings in the horizontal direction.

Simpson<sup>26</sup> used USM3d to compare developed pitch and yawing moments on a Mk-82 500lb bomb from the ATFLIR pod and from the geometrically different and physically larger Litening pod, with both targeting pods mounted externally on the fuselage of a F/A-18C. Both the CFD simulations and limited wind tunnel testing<sup>27,28</sup> show that the Litening pod, as compared with the physically smaller ATFLIR, has reduced pitch and yaw moments on a Mk-82 bomb released and descending from an adjacent under wing pylon. In Simpson's study the aircraft with the ATFLIR used a 7.6m tetrahedral simulation while the aircraft with the Litening pod was modeled with 12.7m

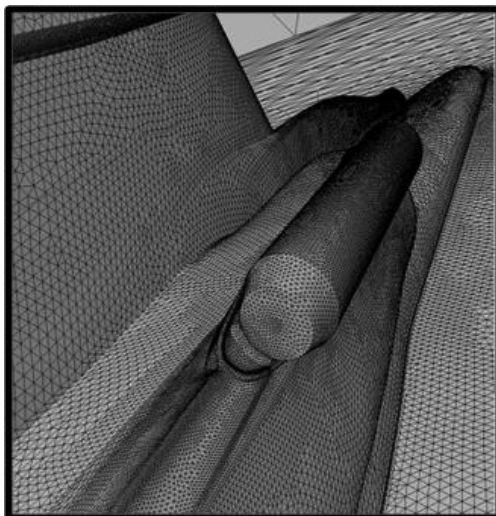


Figure 3. Original.

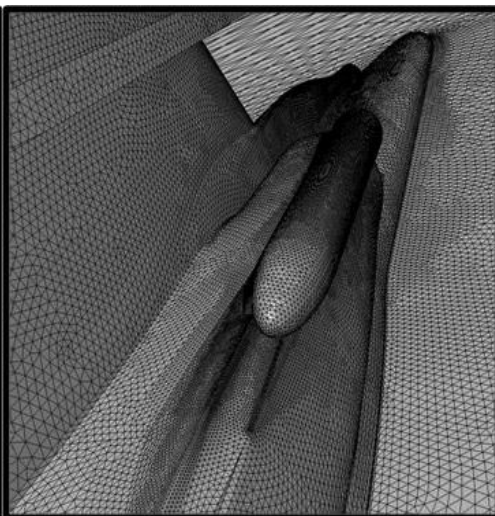


Figure 4. Version 2.

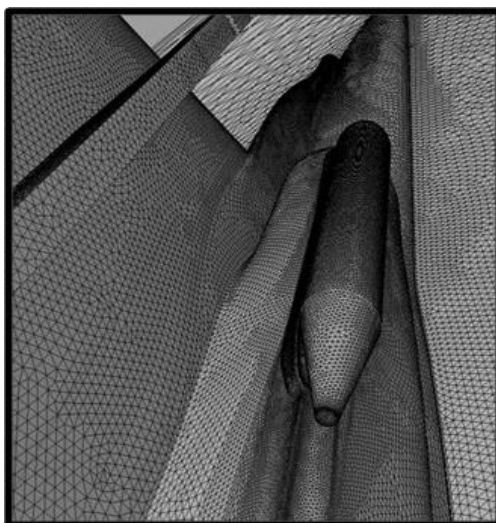


Figure 5. Version 3.

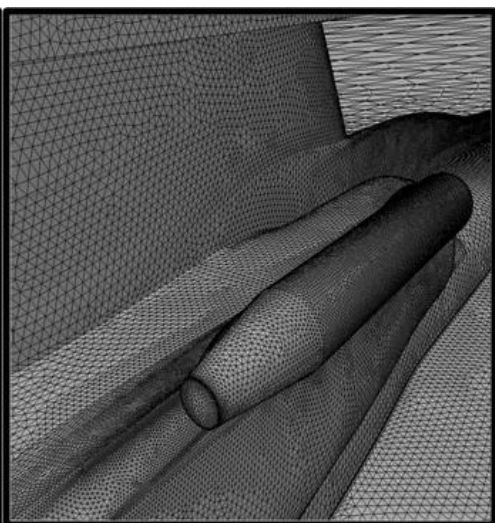


Figure 6. Version 4.

tetrahedral. Both simulations used a wall function boundary layer formulation<sup>(15)</sup> with the Spalart-Allmaras<sup>(21)</sup> single equation turbulence model, the latter which was also used in the S-3B SLAM ER study where CFD/6-DOF trajectories compared well with flight test trajectories<sup>(19)</sup>. Although Simpson's CFD simulation store moments did not exactly match the wind tunnel test data, the trends in moments did show general correlation (e.g. positive moment increasing with increasing Mach). Some of the error could possibly be attributed to comparison of wind tunnel results from two different wind tunnels that are different in size and scale (with aircraft models of different scale), and using a plane of symmetry model of the aircraft in one of the tunnels. Also, the aircraft models were modified to affix the balance from each wind tunnel.

Finally, in an analysis similar to that used herein, Shea<sup>(29)</sup> used USM3d to show that repositioning an external air cooling intake scoop on the Litening Pod could improve the store separation

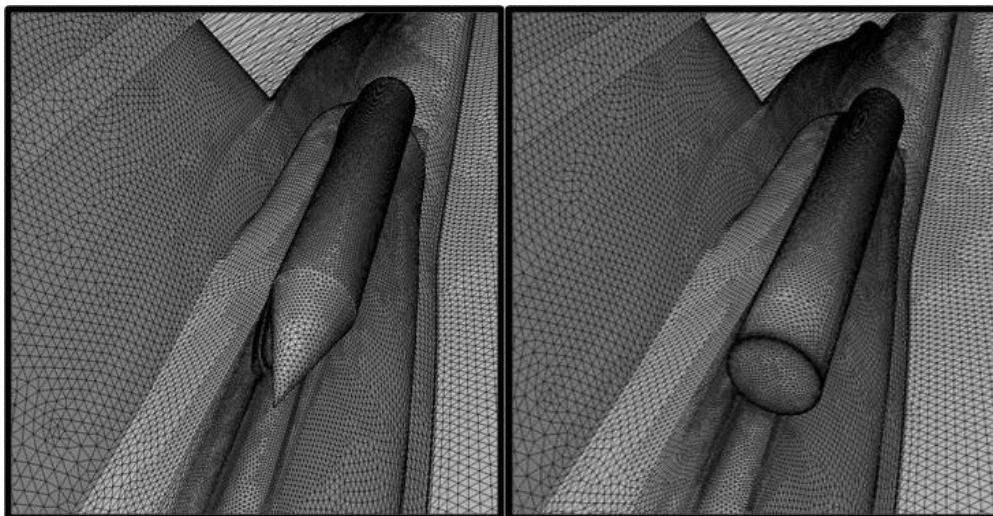


Figure 7. Version 5.

Figure 8. Version 6.

characteristics for a Mk-83 1,000lb gravity bomb released from an F/A-18C in the range  $0.8 \leq \text{Mach} \leq 0.98$ . For an F/A-18C in a  $60^\circ$  dive at Mach 0.94 and 11,400ft, minimum miss distance was increased from approximately 3 to 6 inches. However, and similar to this study, validation of Shea's results via wind tunnel testing was recommended.

## 5.0 GEOMETRY MODIFICATIONS

Because the problems with stores separation were believed to originate from the trailing end of the ATFLIR pod, different modifications in geometry were proposed to the trailing end in order to improve its properties. The six geometries studied are shown in Figs 3-8.

The original ATFLIR geometry, Fig. 3, has an abrupt though slightly tapered end which may cause increased drag and more severe shock waves. Version 2, Fig. 4, is an ogive, which is typically used as the streamlined face of a bullet or artillery shell. While aerodynamic, it may be difficult to produce and thus several simpler cone versions were proposed. Version 3, Fig. 5, is a cone truncated at the aft most end, Version 4, Fig. 6, is also a cone but with more truncation while Version 5, Fig. 7, is an un-truncated cone. Version 6, Fig. 8, with an abruptly truncated aft section, is similar to the Litening pod. The Litening pod, which is significantly longer than the ATFLIR, is known to have less adverse store separation characteristics than the ATFLIR, as shown both in wind tunnel testing and CFD simulations<sup>(1,25,26)</sup>.

## 6.0 FLOW SIMULATION

Numerical simulations of the transonic flow fields herein were performed using the NASA USM3d flow solver. Geometry representing a symmetric half of an F/A-18C equipped with an ATFLIR mounted on the starboard side of the aircraft and a released Mk-82 was created using Rhino, a versatile computer aided design (CAD) program compatible with TetrUSS. An unstructured three-dimensional grid was then generated around the CAD model (associated surface grid shown in Figs 3-9). The unstructured grid allows for finer resolution where greater

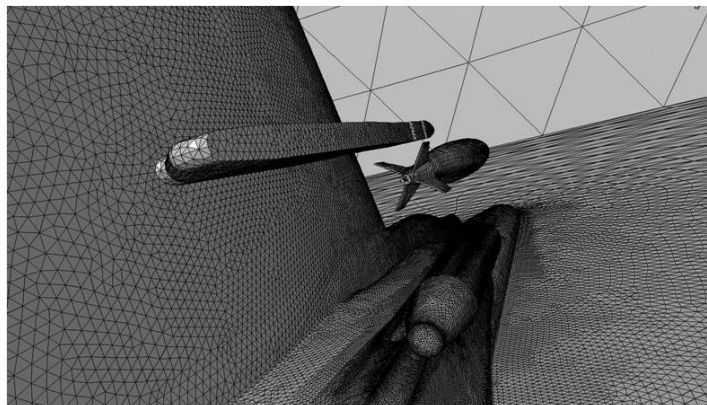


Figure 9. Surface grid of varying resolution.

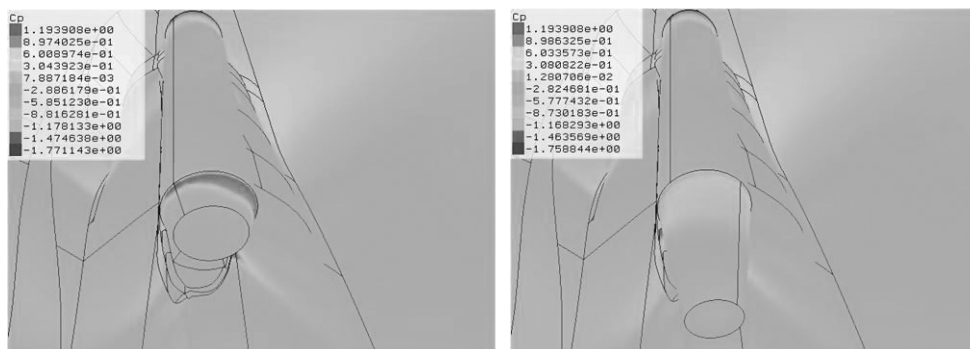


Figure 10. Original (left) vs version 4 (right) pressure distribution.

variation in air flow is expected. Different grids were generated for various prospective tail sections on the ATFLIR.

All simulations were performed at a zero angle of attack, since this typically has been the most limiting case for store separation from the F/A-18C<sup>(1)</sup>. Since we were interested in incremental changes in moments on the released Mk-82 due to changes in the ATFLIR aft geometry, and to simplify calculations, air flow through the starboard side aircraft engine was not modeled in these simulations.

The grids for the ATFLIR were initially divided into approximately 12.7-m tetrahedrals, each of varying size and generated from the underlying surface grid. A second set of grids of approximately 19.7-m tetrahedrals were also used as part of a subsequent grid refinement study. The tetrahedral grids were divided into partitions to allow parallel processing on the US Naval Academy (USNA) Thresher cluster. Simulations were performed using a full viscous or a wall function boundary layer<sup>(15)</sup>, both with Spalart-Allmaras<sup>(21)</sup> single equation turbulence model.

Moments on the released Mk-82 bomb were calculated by USM3d while flow visualisation was done using TecPlot and EnSight visualisation software.

For the 12.7-m tetrahedral grid a given solution would take approximately 32 hours to converge on eight processors, for a total time of approximately 256 processor hours per solution. Convergence was noted when the log of average residuals, or change in flow conditions in a given tetrahedral between iterations, decreased by approximately  $-2.0$  (or flow variation between computational iterations had decreased to approximately 1% of the initial variation). Simulations



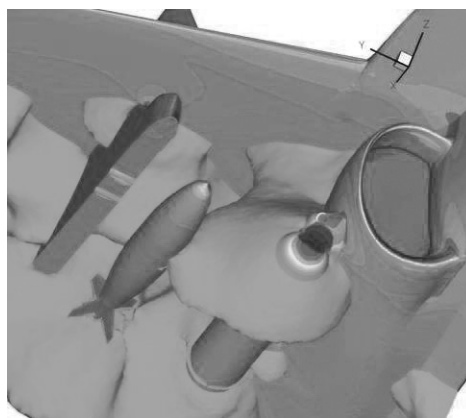


Figure 11. ATFLIR on F/A-18C.

were repeated for each ATFLIR version for  $0.8 \leq \text{Mach} \leq 0.98$  using the full viscous boundary layer model. Simulations were repeated for Versions 2 and 4 at Mach 0.85, 0.90 and 0.95 using the wall function boundary layer. Additional simulations were done for Versions 2 and 4 with the 19.7m tetrahedral grid using the full viscous boundary layer at Mach 0.85, 0.90 and 0.95. The 19.7m tetrahedral grid solutions required approximately 500 processor hours to converge. Total processor hours required were approximately 24,500.

## 7.0 ANALYSIS METHOD

In order to select the most promising versions for additional analysis, initial comparisons were made of the overall drag coefficient  $C_D$  exhibited by each ATFLIR version over the Mach range studied. This analysis is based on the assumption that  $C_D$  is an indicator of the pressure gradient on the trailing end, and thus an indicator of the severity and angle of incidence of the shock wave. This effect can be shown in the comparison of the original ATFLIR and Version 4 in Fig. 10. The less shading on the modified version indicated a lower pressure, and thus a lower drag. Because the shock wave is formed by a difference in pressure, this pressure and drag difference is often a good indicator of the intensity and angle from the ATFLIR that the shock wave will form.

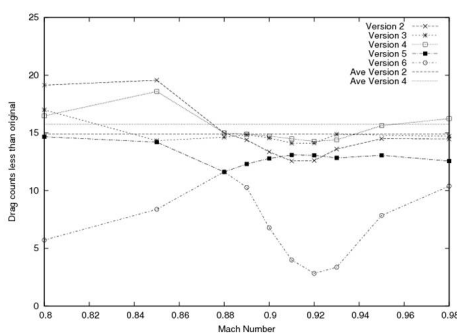


Figure 12. Improvement in drag counts over original ATFLIR vs Mach.

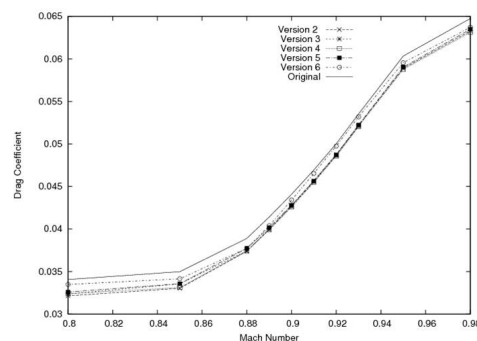


Figure 13. Drag coefficient vs Mach for original and modified ATFLIR.

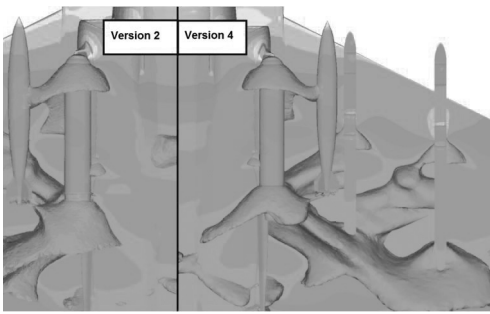
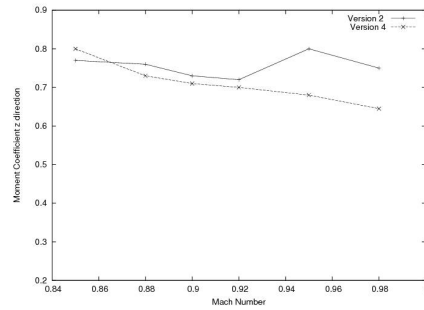
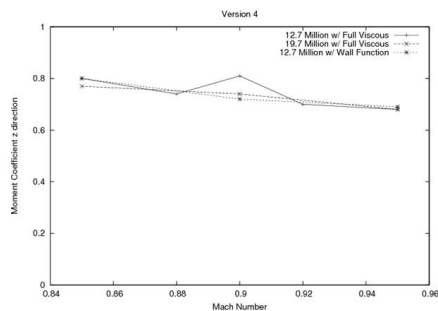
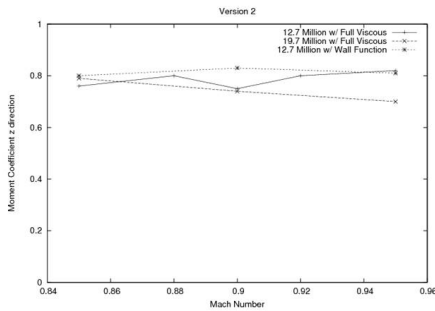


Figure 14. Formation of shockwave.

Figure 15. z direction moment coefficient ( $C_{m_z}$ ) vs Ma.Figure 16. z direction moment coefficient ( $C_{m_z}$ ) vs Ma for Version 2 (left) and Version 4 (right).

Previous studies<sup>(1,25,26,28)</sup> have shown that the main source of adverse store separation characteristics stems from the blunt aft section of the pod. This part of the pod can generate a shockwave that hits the tail of the store, which can cause a detrimental yawing moment and thus, potentially, a collision between the store and aircraft. Visualisation from underneath a F/A-18C with an ATFLIR and a released Mk-82 is provided in Fig. 11. In this view it is clear that the shockwave from the nose of the ATFLIR strikes the store in the middle of its body, whereas the shockwave from the aft of the pod strikes close to the fins of the Mk-82. This flow visualisation shows how the shock wave from the aft section of a targeting pod, which was previously thought to be inconsequential, can have a large effect on the store separation properties.

## 8.0 RESULTS

A 'Mach sweep' for all versions was conducted using the 12.7m tetrahedral grid with a full viscous boundary layer. The resultant  $C_D$  were then calculated and compared. Figure 12, which shows incremental improvement in  $C_D$  over the original ATFLIR, as measured by drag counts (one drag count = .001 change in  $C_D$ ) indicates that all modifications produced less drag at all Mach than the original version. The more positive the number shown in Fig. 12, then the greater the improvement in drag counts over the original aft end configuration. In Fig. 12 the average of Version 2 and Version 4 are also shown as horizontal lines. An average  $C_D$  over all Mach analysed was used to determine the best versions, although future work may want to put more emphasis on a specific Mach range that is more critical to the aircraft flight envelope. From this analysis it was determined that Version 2 and Version 4 were the two most promising modifications, with

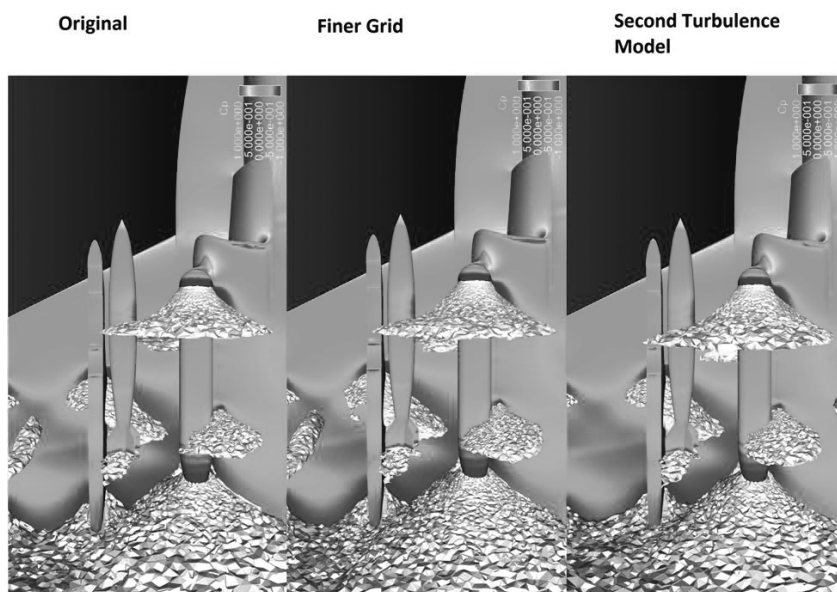


Figure 17. Flow visualisation at Ma 0.85 for original grid (left), finer grid (centre) and original grid with second turbulence model (right).

Version 4 having slightly less drag than Version 2, especially at higher Mach. Figure 13 shows the drag coefficient as the Mach is increased. This figure shows the general behavior that would be expected and helps to validate the results.

This reduction in overall drag by itself may be enough to justify ATFLIR aft end modifications. The fuel savings from the decrease in drag could justify the addition of a tail cone to minimise the formation of adverse trailing end shock waves. The modification thus has the potential to both reduce aircraft fuel consumption and improve the store separation characteristics of the ATFLIR.

Version 2 and Version 4 were then investigated further. The computational space was altered, inserting an Mk-82 store just released from the inboard pylon carriage position as shown in Fig. 9. This position is the point where the expected maximum interference between the shockwave and Mk-82 will occur. A Mach sweep of both versions was conducted in this configuration. The shock waves emanating from the store were visualised, and the moment coefficient on the Mk-82 was extracted. The position of the store relative to the aircraft can also be seen in Fig. 11, which is a view from below the F/A-18C.

The shockwave emanating from the two different versions are shown in Fig. 14. The shockwave from the leading end of the ATFLIR is shown to intersect the store at about midsection. This would not cause a large moment on the store and is not thought to generate an adverse moment that could cause the store to contact the aircraft. However, the shockwave from the trailing end intersects the store close to the tail of the Mk-82. This would cause a large moment on the store and cause it to rotate, possibly into the aircraft.

As shown in Fig. 14, the shockwave emanating from Version 2 is slightly closer to the fins of the store than the shockwave from Version 4. It can be seen that the shock wave from the tail end of Version 2 emerges at an angle greater than that of Version 4, and interferes more with

the Mk 82. Of interest is that the shockwave from Version 2 starts further aft, it departs at a more oblique angle to the ATFLIR, and comes closer to the fins of the Mk-82. This indicates that Version 4 performs better.

The moment coefficient on the store was also obtained from the simulations. The  $z$  direction moment coefficient  $Cm_z$  is plotted against Mach in Fig. 15. Figure 15 indicates that Version 4 interferes less with the store than Version 2. Both versions have similar behavior at low Mach. However, at Mach 0.96 and 0.98, Version 2 creates a moment on the store that is approximately 10-15% greater than that from Version 4.

## 9.0 GRID REFINEMENT AND BOUNDARY LAYER SIMULATION STUDY

In order to help validate the comparison between Versions 2 and 4, additional simulations were performed using a finer unstructured grid (19.7m tetrahedrals) and with the original 12.7m tetrahedral grid but with a wall function boundary layer instead of a full viscous boundary layer model. Sample results are shown in Fig. 16, which compares  $z$  direction moment coefficient  $Cm_z$  vs Mach for the different cases analysed. For both versions  $Cm_z$  shows consistent trends between the three sets of simulations. Similar results were obtained for  $Cm_x$  and  $Cm_y$ .

Comparison can also be made in flow visualisation between the three sets of simulations. Figure 17 compares the shock waves between the 12.7m tetrahedral grid with full viscous boundary layer, the 19.7m tetrahedral grid with full viscous boundary layer and the 12.7m tetrahedral grid with wall function boundary layer, all at Mach 0.85. Figure 17 clearly shows nearly identical shock waves present in all three simulations. Figure 17 visualisations are consistent with similar trends in  $Cm_x$ ,  $Cm_y$  and  $Cm_z$  obtained in the three different sets of numerical simulations.

## 10.0 CONCLUSIONS

Our numerical simulations show that Version 4 has less overall drag than Version 2. Version 4 also produced a smaller moment on the Mk-82, especially at higher Mach. By visual inspection of the shock wave, Version 4 also has qualitatively better performance which correlates with the calculated moment coefficients. Consequently, Version 4 has been predicted to reduce adverse store moments better than Version 2.

This result is counter to what was originally expected. It was assumed that the smoother ogive shape, which has been designed to reduce drag in artillery shells and rockets, would produce the better performance. However, the simpler and easier to manufacture version appears to perform better. These results should be compared to wind tunnel test data of the modified ATFLIR. This could be used to determine whether the calculations performed were valid with possible eventual implementation of the modification.

## ACKNOWLEDGMENT

A portion of this research was performed while then Midshipman O'Brien was a summer intern at the Maui High Performance Computing Center. The summer internship was funded by the Department of Defense High Performance Computing Modernization Program Office.

## REFERENCES

1. GODIKSEN, W. Effects of targeting pods addition on F/A-18C Hornet weapons release, 2008, AIAA 2008-6380: Atmospheric Flight Mechanics Conference and Exhibition, 2008, Honolulu, Hawaii, USA.
2. ROGERS, R. A comparison between the Nielson and Woodward programs in predicting flow fields and stores loads, 1976, Naval Weapons Center TM2854.
3. CENKO, A. and TINOCO, E., PAN AIR – weapons, carriage and separation, 1979, Air Force Flight Dynamics Laboratory TR-79-3142.
4. STEGER, J., DOUGHERTY, F. and BENEK, J. A Chimera grid scheme, Advances in grid generation, 1983, American Society of Mechanical Engineers Fluids Engineering Conference, 1983, Houston, Texas, USA.
5. CENKO, A. Store separation lessons learned during the last 30 years, 2010, ICAS 2010-2.11ST1, 27th International Congress of the Aeronautical Sciences (ICAS), 2010, Nice, France.
6. KEEN, K. Inexpensive calibrations for the influence function method using the interference distributed loads code, *J Aircr*, January 1985, **22**, (1), pp 85-87.
7. CENKO, A., MEYER, R. and TESSITORE, F. Further development of the Influence Function Method for store aerodynamic analysis, *J Aircr*, August 1986, **23**, (8), pp 656-661.
8. CENKO, A. and LUTTON, M. ACFD application to store separation – status report, *Aeronaut J*, October 2000, **104**, pp 459-466.
9. WALSH, J. and CENKO, A. USM3D Prediction of Mk-83 trajectories from the CF-18 Aircraft, 2001, AIAA 2002-2431, 19th Applied Aerodynamics Conference, 2001, Anaheim, CA, USA.
10. RYCKERBUSCH, C., NIEWOEHNER, R., CENKO, A., SISCO, B. and WALSH, J. Evaluation of the capabilities of CFD to predict store trajectories from attack aircraft, 2002, AIAA 2002-0279, 40th Aerospace Sciences Meeting, 2002, Reno, NV, USA.
11. CENKO, A., NIEWOEHNER, R. and RYCKERBUSCH, C. Evaluation of the capabilities of CFD to predict store trajectories from attack aircraft, 2002, ICAS 2002-2.6.1, 23rd International Congress of Aeronautical Sciences, 2002, Toronto, Canada.
12. FRINK, N. Upwind scheme for solving the Euler equations on unstructured tetrahedral meshes, *AIAA J*, January 1992, **30**, (1), pp 70-77.
13. FRINK, N. Recent progress toward a three-dimensional unstructured Navier-Stokes flow solver, 1994, AIAA 1994-0061, 32nd Aerospace Sciences Meeting and Exhibition, 1994, Reno, NV, USA.
14. FRINK, N. Tetrahedral unstructured Navier-Stokes method for turbulent flows, *AIAA J*, November 1998, **36**, (11), pp 1975-1982.
15. FRINK, N., PIRZADEH, S., PARIKH, P., PANDYA, M. and BHAT, M. The NASA Tetrahedral Unstructured Software Systems (TetrUSS), 2000, ICAS 2000-2.4.1(IL), 22nd International Congress of Aeronautical Sciences, 2000, Harrogate, UK.
16. WELTERLEN, T. and LEONE, C. Application of viscous, Cartesian CFD to aircraft store carriage and separation simulation, 1996, AIAA 1996-2453, 14th Applied Aerodynamics Conference, 1996, Denver, CO, USA.
17. WELTERLEN, T. Store release simulation on the F/A-18C using split flow, 1999, AIAA 99-0124, 37th Aerospace Sciences Meeting and Exhibition, 1999, Reno, NV, USA.
18. CENKO, A.T., CENKO, A.T., PIRANIAN, A. and DENIHAN, S. Utilizing flight test telemetry data to improve store trajectory simulations, 2003 AIAA 2003-4225, 21st Applied Aerodynamics Conference, 2003, Orlando, FL, USA.
19. RAY, E. CFD method for separation of SLAM-ER from S-3B, 2003, AIAA 2003-4226, 21st Applied Aerodynamics Conference, 2003, Orlando, FL, USA.
20. JESPERSEN, D., PULLIAM, T. and BUNING, P. Recent enhancements to OVERFLOW, 1997, AIAA 1997-0644, 35th Aerospace Sciences Meeting and Exhibition, 1997, Reno, NV, USA.
21. SPALART, P. and ALLMARAS, S. A one-equation turbulence model for aerodynamic flows, 1992, AIAA 1992-0439, 30th Aerospace Sciences Meeting and Exhibition, 1992, Reno, NV, USA.
22. CENKO, A. One CFD calculation to end point flight testing (has CFD finally replace the wind tunnel?), *Aeronaut J*, July 2006, **110**.
23. CENKO, A. Lessons Learned in 30 years of store separation testing, 2009, AIAA 2009-98, 47th Aerospace Sciences Meeting, 2009, Orlando, FL, USA.
24. SNYDER, M., SHAH, R., O'BRIEN, C., DAVIS, N., METZGER, J., NORDLUND, R. and SMITH, M. Strut effects on store freestream aerodynamics, 2011, AIAA 2011-3159, 29th Applied Aerodynamics Conference, 2011, Honolulu, HI, USA.
25. GODIKSEN, W. and HALLBERG, E. Targeting pod effects on weapons release from the F/A-18C, 2008, ICAS 2008-2.9.4, 26th Congress of International Council of the Aeronautical Sciences, 2008, Anchorage, AK, USA.
26. SIMPSON, S., SNYDER, M. and CENKO, A. Effects of the Litening and ATFLIR external targeting pods on F/A-18C Hornet weapons release, 2011, AIAA 2011-3157, 29th Applied Aerodynamics Meeting, 2011, Honolulu, HI, USA.
27. VEAZEY, D. and HOPF, J. Comparison of aerodynamic data obtained in the Arnold Engineering Development Center wind tunnels 4T and 16T, 1998, AIAA Paper 1998-2874, 20th Advanced Measurement and Ground Testing Technology Conference, 1998, Albuquerque, NM, USA.
28. DROBIK, J. and LAM, S. Validation of plane of symmetry testing in the DSTO 0-8m wind tunnel, 2010, International Test and Evaluation Association, 15th Aircraft/Stores Compatibility Symposium, Fort Walden Beach, 2010, FL, USA.
29. SHEA, M., CONSTANTINO, M., O'BRIEN, C., SNYDER, M., SIMPSON, S. and CENKO, A. Litening Pod modification to improve Mk-83 trajectories, 2011, AIAA 2011-3158, Applied Aerodynamics Conference, 2011, Honolulu, HI, USA.